Vol. 07, No. 01, pp. 223 –231 (2026)
ISSN: 2708-0757

JOURNAL OF APPLIED SCIENCE AND TECHNOLOGY TRENDS

www.jastt.org

Road Network Index: A Novel Spectral Index for Urban Road Network Extraction from Landsat Imagery

Yashwant Soni[1], Uma Meena[1,*], Vikash Kumar Mishra[2]

[1]*Department of Computer Science and Engineering, SRM Institute of Science and Technology, Delhi-NCR Campus, Modinagar, Ghaziabad, Uttar Pradesh, India, yashalw80@gmail.com, uma.b18@gmail.com*
[2]*School of Computer Science and Engineering, Galgotias University, Greater Noida, Uttar Pradesh, India*
mail2dr.vikash@gmail.com

**Correspondence: uma.b18@gmail.com*

Abstract

Urban road information extraction from low- to medium-resolution remote sensing imagery remains challenging due to the limited spectral separability between road surfaces and surrounding urban features. This work proposes a road network index (RNI), a novel spectral index for urban road network extraction, to delineate the urban road network from Landsat satellite imagery. In the first step, the Landsat data is pre-processed to handle the atmospheric correction followed by the selection of the spectral bands used to develop RNI by performing spectral analysis. The proposed RNI is used for the identification of road information from Landsat imagery, and the road and non-road information is separated using thresholding. Furthermore, the non-road components are eliminated by using geometric feature analysis. By applying RNI to Landsat multispectral imagery, we can extract urban road networks accurately and efficiently. Results reveal that RNI is automated, convenient in asphalt road extraction from medium-resolution satellite imagery. Experimental results demonstrate that the proposed approach achieves an overall accuracy of 91.67%, a Kappa coefficient of 0.8334, and an F1-score of 91.64%, indicating strong agreement and balance between precision and recall. These findings confirm that RNI provides an automated and reliable solution for asphalt road extraction from medium-resolution satellite imagery, particularly in complex urban environments.

Keywords: *Road network index, Landsat imagery, road extraction, urban road, remote sensing, Urban*
Received: January 14th, 2026 / Revised: March 30th, 2026 / Accepted: April 12th, 2026 / Online: April 19th, 2026

I. INTRODUCTION

Road networks have been a key part of human society since ancient times. They are important for many things, such as urban planning, managing transportation, and dealing with disasters [1]. Road network information can be obtained from remote sensing images (RSI), such as satellite and aerial images. However, road network extraction from RSI has been a challenging and extensive research area since the evolution of RSI technology due to various factors like low spectral variability between different contextual objects present in satellite imagery, variation in spatial resolutions, heterogeneous land cover surface, noise and various occluding factors [2]. The imaging quality of RSI depends on seasons, road surface conditions and spatial resolution. Furthermore, the road networks are complex having varying widths, curvatures, and intersection patterns that pose hurdles in delineating road segments, especially in densely populated urban areas from satellite imagery [3]. The automatic delineation and vectorization of the road network from RSI is a tough and tedious task.

RSI can be categorised into low, high and medium resolution based on the spatial resolution it has [4]. Low-resolution RSIs are unsuitable for urban road information extraction as the information in low-resolution (>30m) images is insufficient as roads may have widths less than the spatial resolution available. At the same time, the high (<5 m) or medium-resolution (MR) (5-30 m) images are primarily suitable for urban road network information extraction. High resolution satellite images (HRSI) are widely used to delineate road network information as they have precise road information [5], [6]. However, the use of HRSI for large-scale road extraction is hindered by its limited coverage area, infrequent revisit times, and high cost. Recent research has shifted towards using MR imagery from satellites like Landsat and Sentinel-2 [7] for road network detection. This is due to their free availability, global coverage, and more frequent revisit times compared to HRSI and offers the potential

doi: 10.38094/jastt71788

to extract roads from MR images. The Landsat-8 is a multispectral satellite and provides images of spatial resolution to 15-30 m. Road information extraction from MR imagery is very challenging, especially in urban areas due to the presence of shadows of occluding factors such as trees, multistorey buildings, and flyovers constructed along the roadside. Furthermore, the roads are generally built with various types of materials (a combination of Asphalt and crushed stones, charcoal etc.) that alter the road surface's spectral reflectance and pose hurdles in road delineation from RSI [8]. Various methods of road network extraction from MR imagery have been proposed in the literature and are mainly based on the use of classification [9], [10], knowledge-based or road feature-based [11] and Spectral index-based methods [12], [13]. For extracting road networks from MR imagery, the classification-based techniques based on machine learning models like SVM [14], ANN [15], and random forest [16] have lower performance than deep learning models. These methods cannot handle the issues of low spectral variability and occluding effects. On the other hand, the DL-based techniques require a enormous quantity of labelled data for the training which makes them computationally inefficient for road network delineation tasks [17], [18], [19]. Similarly, road feature-based methods are computationally expensive, require human intervention in seed point selection suffer from the issue of over-segmentation and are suspectable to occlusions [20]. The objective of our study is to extract urban road networks from MR Landsat-8 imagery of a densely populated area.

A major challenge in delineating road networks from urban areas using RSI is the discrimination of roads from other objects having similar radiometric properties as they have overlapping spectral signatures, especially in visible and NIR bands. This overlapping can lead to high false positives from buildings, parking lots, and other impervious surfaces. Existing indices-based methods are designed using fixed spectral band combinations without any rigorous justification, which often leads to poor generalization when roads and built-up areas exhibit similar material properties. Furthermore, the magnitude and directional behaviour of spectral variation between adjacent NIR and SWIR bands, which contains significant information for separating linear road features from areal built-up regions, has not been sufficiently exploited. Furthermore, the segmentation-based methods increase computational complexity and limit scalability for large-area mapping.

To address all these challenges, in this work a Road network index (RNI) is designed by using the distinct reflectance difference between NIR (Band 5) and SWIR-1 (Band 6), identified through spectral reflectance curve analysis. The normalization of these bands further facilitates the identification of the minor spectral differences between them which can be used to identify road–built-up separability while maintaining computational efficiency. The development of RNI fills the gap between existing spectral indices and computationally intensive traditional methods, providing a precise and accurate solution for urban road network extraction. The proposed method can delineate road networks from heterogeneous land cover surfaces by eliminating non-road structures with road-like radiometric properties. The main points and contributions of this research work are as follows:

(i) A computationally efficient automatic method for urban road network delineation from MR imagery without the large, labelled dataset required for deep learning and machine learning-based methods.

(ii) Development of road network index (RNI), a novel spectral index for urban road network extraction, to delineate the urban road network from Landsat satellite imagery.

(iii) For designing of RNI band Selection is performed by the spectral analysis of Landsat Imagery.

(iv) Verification of the extracted road network from Google Earth images

The remaining paper is structured as follows: the existing methods of road network extraction from MR Landsat images are discussed in Section II. The dataset and proposed methodology are described in Section III followed by the experimental results and their verification from Google Earth images in Section IV. Finally, the conclusion and future aspects of the work are discussed in Section V.

II. Related work

Existing methods for delineating road networks from MR satellite imagery can be categorized into Road features-based, classification-based, and spectral index-based methods.

A. Road feature-based methods

Most road network delineation methods use only their local and texture features that can be altered by various occluding factors. The complex stripe structures of roads make it difficult to use as a feature vector for classification as road and non-road. A road delineation technique based on a snake for extracting stripe-like linear structures is designed that use energy functions to track the road until it converges [21]. The geometric features of the road network are integrated into a road model, followed by applying dynamic programming to solve this model using the merit function [22]. The road-tracking mechanism is used to extract the road network from RSI by creating a template window around a seed pixel, followed by a matching of the geometric features of the road network [11]. These methods are generally semi-automated due to the selection of initial seed pixels, time-consuming and are unable to handle the occluding factors.

B. Classification-based methods

The classification-based method segments the RSI into road and non-road components by using the photometric and texture features of roads followed by post-processing operations such as mathematical morphology to eliminate the false road components. These methods can be broadly divided into traditional segmentation-based, machine-learning and deep learning-based methods. Traditional segmentation techniques, such as region-growing [23] and threshold-based approaches, are used to identify road networks from the RSI. However, due to low spectral variability, traditional methods are inefficient in delineating road networks from MR resolution. Machine learning techniques have been widely used in identifying urban objects from MR resolution imagery in the last decade. The different features of images like texture, edge, colour etc are

used to train the classifiers and the trained model is used to detect road information. Texture features are used to identify road information from Landsat-8 imagery using SVM [14] and random forest [16] and colour features have been used to delineate road networks from MR imagery using ANN [15]. SVM in combination with the level set and morphological method is used to delineate the road network from multi-sources RSI of world view, Ultracam and QuickBird satellite [24]. But the proposed method is unable to handle the issues of uneven width, complex heterogenous land cover and complex road junctions.

The pixel-based classification method generally has a higher rate of misclassification because the road network and other building structures are made up of identical material, and due to the low spectral variation between road and non-road pixels, the non-road component is also considered as road. To eliminate such issues, the geometric properties such as area, aspect ratio, etc., of the road network are efficiently used and are implemented using mathematical morphological operations.

The road network extracted by the classification-based methods suffers from the issue of a broken network due to the variation in spectral properties of the road network caused by the shadow of the trees and building infrastructures present alongside the road network. To handle all these challenges, various techniques have been proposed by the researchers. The first step in these methods is to resolve the issue of road uneven width, which means the road network is sleek. After that, techniques like tensor voting [25], maximum response filtering using Gabor filter [3] and morphological operations [26] and are widely used to resolve this issue. Liu et al. have used shear transform and directional morphological methods for delineating smooth and sleek road centrelines from HRSI [27]. Shi and Debayle have designed a multistage road network to delineate complete and accurate road centrelines from HRSI [28]. In the first stage of the method, the road region is identified using the SVM method, followed by the elimination of false road components using shape feature analysis and the road centerline is identified by using a regression-based technique. Various techniques have been designed to extract the road centreline or sleek road network from RSI, but their performance depends on the classification method used to find the initial road network.

In recent years, deep learning-based CNN architectures have been widely used in computer vision tasks such as feature extraction, object segmentation, and object detection. U-Net-based CNN architecture is used to monitor and delineate road information of the Congo Basin from multi-sensor MR resolution multi-sensor data [18]. A 3D CNN architecture is employed as a feature extractor, followed by a multi-class SVM as a classifier used to extract developed urban classes from multi-temporal Landsat-8 imagery [19]. Singh and Tyagi [17] designed a CNN architecture with five hidden layers and seven training features to classify the Landsat 8 imagery.

C. Spectral index-based Road Extraction methods

Spectral index-based road extraction methods have been widely used to extract information about built-up contextual objects like roads, buildings, etc., from multispectral imagery. Band 3 and Band 4 of the Landsat TM imagery are used to design the Normalised Difference Vegetation Index (NDVI) for extracting build-up areas [29]. Similarly, the normalised difference built-up index (NDBI) is developed using Bands 4 and 5 of the Landsat TM imagery to identify built-up areas [30]. These methods are inefficient in extracting road information due to the variation in spectral responses of roads. To handle these challenges Mhangara et al.[31] have designed the built-up area index (BAI) using the Blue and Near-infrared band (NIR) to delineate road and built-up areas from multispectral aerial imagery. Shahi et al.[13] has improved BAI and proposed road extraction index (REI) to delineate asphalt roads from multi-spectral WorldView-2 imagery using Blue and NIR bands. Reddy et al.[12] has designed a road index (RI) by using SWIR 1, NIR, blue and red bands to extract road information from Landsat-8 OLI images. The existing indices shown in Table I are implemented on various types of imagery and they are specific to only that type of imagery or sensors and are unable to detect road networks of different types of materials. However, the road information extracted by RI required further processing using the Markov random field (MRF) technique. Ahmed et al. [32] used the RI on the Sentinel-2 dataset to delineate road networks. The formulation of various existing road indices is presented in Table I.

TABLE I. FORMULATION OF EXISTING ROAD INDICES

Author	***Index***	***Bands and Subsets***	***Purpose***
Shahi et al.[13]	$REI = \frac{NIR2 - BLUE}{NIR2 + BLUE \times NIR2}$	Blue and NIR2 World view-2	Asphalt road extraction
Mhangara et al.[31]	$BAI = \frac{BLUE - NIR}{BLUE + NIR}$	Blue and NIR Multispectral Aerial	Roads and Built-up Area
Reddy et al[12]	$RI = \frac{3 \times min(SWIR1, BLUE, NIR}{(SWIR + NIR + BLUE)}$	SWIR, BLUE, NIR Landsat-8 OLI	Road information

III. DATASET AND PROPOSED METHODOLOGY

In this section, the descriptions of the study area, dataset and method used to formulate the RNI to delineate the road network are discussed.

A. Study area and dataset

The study area selected for this research is Las Vegas city, Nevada, United States, geographically bounded by the coordinates (36°20′51.79″N, 115°22′47.76″W) and (35°57′7.54″N, 114°56′26.50″W). As one of the fastest-growing urban centers in the country, Las Vegas has experienced substantial population expansion, increasing from approximately 273,000 in 1972 to 2,200,079 in 2017, representing a growth of over 700%. A major consequence of rapid population growth is the transformation of the natural landscape into increasingly impervious urban surfaces. In this study, Landsat imagery acquired in 2018 was utilized to extract the road network of Las Vegas city. The true color composite (TCC) Landsat image of the study area is illustrated in Fig. 1(b).

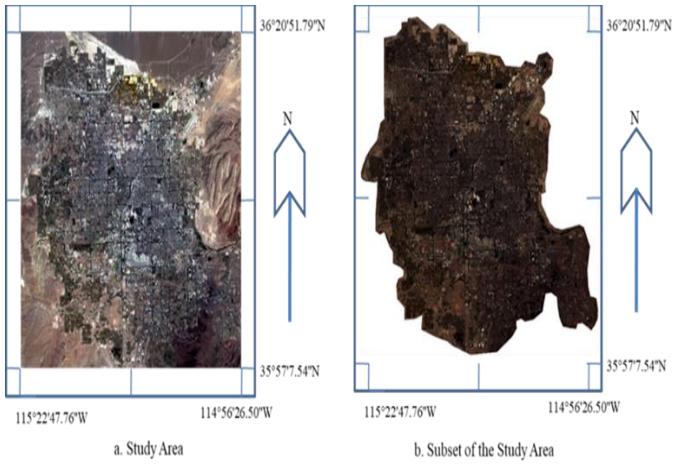

Fig. 1. TCC of the study area from the Year May 2018, (b). Subset of (a).

B. Methodology

The primary goal of the work presented is to extract road networks from Landsat -8 imagery of densely populated urban areas by designing a novel road network index. The flow chart of the proposed method is shown in Fig. 2 and consists of steps namely, preprocessing, band selection using spectral analysis, RNI formulation, post-processing and accuracy assessment.

a) *Preprocessing:* The signal recorded by the sensor mounted on Landsat consists of two components; the actual reflectance from the objects presents on the earth and the noise resulting from atmospheric effects. Before the selection of bands for the calculation of RNI and the images, preprocessing steps namely radiometric correction, layer-stacking, and sub-setting are performed. Radiometric corrections were required to handle the errors in the digital number of the bands, and this was done by converting the data to Top-Of-Atmosphere reflectance (TOA) as per Eq1.

$$q^{\lambda} = \frac{N_q Q_{cal} + A_q}{sin(\theta_{SE})} \quad (1)$$

Where q^{λ} is the TOA planetary reflectance, N_q and A_q is the band-specific rescaling factor from metadata. Q_{cal} is quantized and calibrated product pixel values and θ_{SE} is the sun angle. Furthermore, the bands are stacked together, and the region of the study area is selected from the original imagery as shown in Fig. 2.

b) *Band Selection Using Spectral Analysis:* Four dominant surface features are present from the study area region, namely roads, water bodies, built-up areas, and land. From the satellite imagery, sample pixels corresponding to each class were selected, comprising 850 for roads, 520 for water, 557 for built-up areas, and 484 for land. Using the mean reflectance values of these samples, the Spectral Reflectance Curve (SRC) was generated, as illustrated in Fig. 3. An examination of the SRC leads to the following key observations:

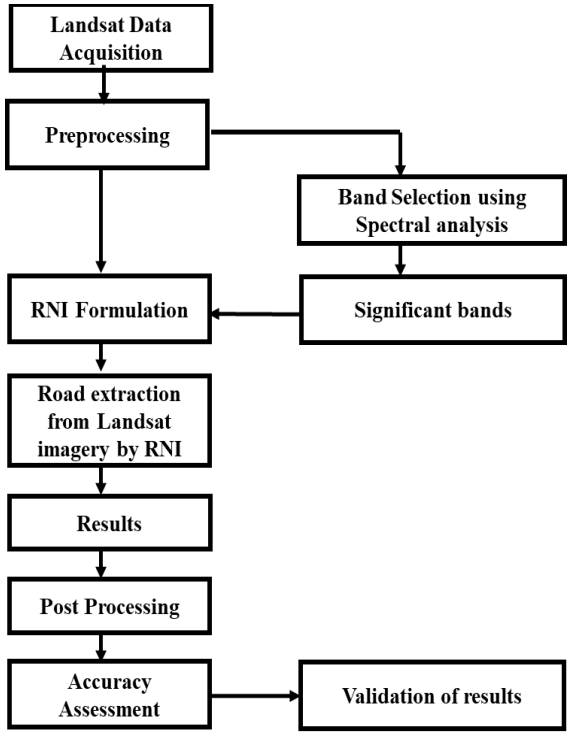

Fig. 2. Flow graph of the proposed method

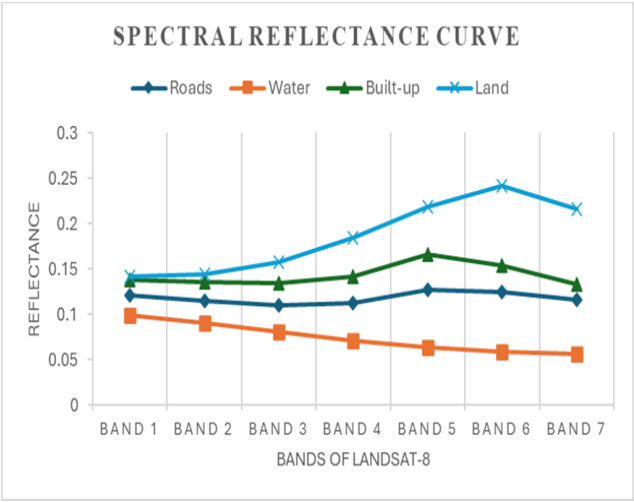

Fig. 3. Spectral reflectance curve

- The reflectance of water consistently decreases from Band 1 through Band 7, indicating an inverse relationship between water reflectance and spectral wavelength.
- The reflectance of land surfaces shows a gradual increase from Band 1 to Band 6, followed by a decline in the subsequent band.
- Roads and built-up areas exhibit comparable reflectance trends across the spectral bands due to

their similar concrete-based composition. However, built-up areas demonstrate higher reflectance values than roads in all bands, except for a slight variation observed between Bands 5 and 6.

- Road surfaces achieve their maximum reflectance in Band 5 and display nearly equivalent reflectance in Band 6. In contrast, the reflectance of built-up areas continuously decreases from Band 5 to Band 7.
- The change in reflectance between Bands 5 and 6 is more pronounced for road features than for built-up regions. Applying a square-root transformation to this difference amplifies distinction, enabling more effective discrimination of road networks from built-up structures.

c) *RNI formulation:* The Road network index (RNI) is formulated by selecting significant bands that capture road information in multispectral Landsat-8 imagery. By performing spectral analysis of different bands of Landsat-8 imagery it has been observed that band 5 (NIR) and band 6 (SWIR-1) best describe the road network. The novel RNI can be formulated by performing an inter-band calculation of band 5 (NIR) and band 6 (SWIR-1) as per Eq. 2. The output by the RNI is a normalized image whose spectral values highlight the road network to other features as shown in Fig. 4

$$RNI = \sqrt{\frac{(Band6-Band5)}{(Band6+Band\ 5)}} \quad (2)$$

The used of square root transformation instead of other transformation for the formulation of RNI further stabilizes the dynamic range of reflectance values and reduces extreme variations caused by bright non-road components. Furthermore, it also significantly enhances the spectral separability between road surfaces and spectrally similar urban features such as built-up areas.

(a)

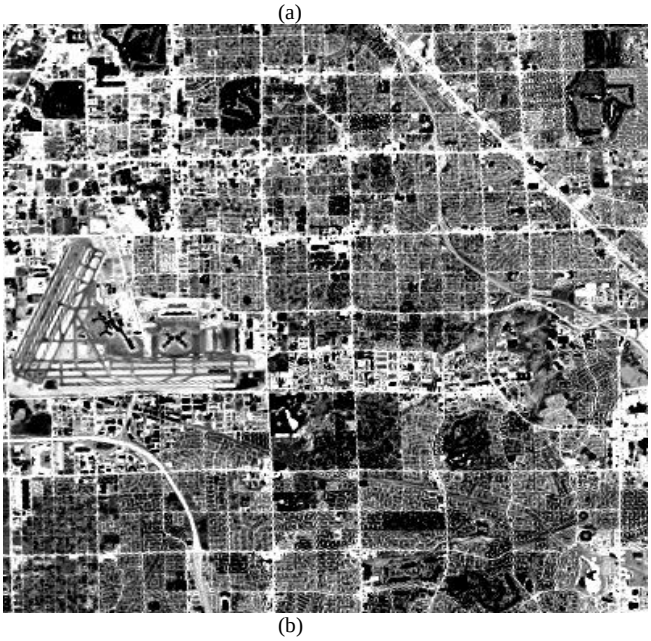

(b)

Fig. 4. Visualization of road network Extracted by RNI having some false road components and on a subset imagery of the study area (a) True color Landsat imagery (b) road network extracted by applying RNI

d) *Post Processing:* The Landsat imagery of the study area has some non-road components along with the road network as shown in Fig. 4(a). A few non-road components, like buildings, have low spectral variation between road and non-road objects detected as roads by RNI, as shown in Fig.4(b). Furthermore, some discontinuities and holes due to the presence of various impeding objects, and temporal effects also degrade the quality of the extracted road network, as shown in Fig. 4(b). To handle all these challenges, first, the road network identified by RNI is enhanced by eliminating small non-road objects by using the Otsu method [33]. The quality of the extracted road network is further enhanced by geometric feature analysis, as roads are long, elongated linear structures that are irregular in their ratio of length and width [34]. These geometric properties of road networks are used to differentiate road components that have road-like spectral responses, such as buildings, structures, etc. The geometric feature analysis is performed by using parameters such as complexity rate (CR) and aspect ratio (AR) as defined in Eq. (3) and (4), which can be calculated by using connected component analysis.

$$CR = \frac{AR}{PM^2} \quad (3)$$

$$AR = max\left(\frac{X_{max}-X_{min}}{Y_{max}-Y_{min}}, \frac{Y_{max}-Y_{min}}{X_{max}-X_{min}}\right) \quad (4)$$

Where AR and PM represent the area and perimeter of the bounding rectangle of the road component. The X_{min} , X_{max} and Y $_{min}$ and Y_{max} represents the

coordinates of the minimum bounding rectangle. The value of CR is set in the range of 30-50 and AR>4. These thresholding values are obtained after extensive experiments, and mathematical formulation is given in Eq (5) - (9) to follow the geometric properties of the road network as road may have different shape and width.

As For a rectangular object with length L and width W

$$CR = \frac{AR}{PM^2} \quad (5)$$

$$AR = L \times W \quad (6)$$

$$PM = 2(L + W) \quad (7)$$

$$CR = \frac{L \cdot W}{[2(L+W)]^2} \quad (8)$$

If the object is road-like (elongated) which means $L > W$:

$$CR \approx \frac{L \cdot W}{4L^2} = \frac{W}{4L} \quad (9)$$

If the object is non-road (square-like) $L \approx W$:

$$CR \approx \frac{L^2}{16L^2} = \frac{1}{16} \times 1000 = 62.5$$

CR is relatively larger which shows that CR naturally distinguishes elongated roads from compact objects. Here CR is scaled (×1000) for numerical stability: Through extensive experiments it has been observed that CR < 30: includes irregular noise and broken fragments, CR > 50: starts including compact regions (false positives). So, CR ∈ [30, 50] gives the best trade-off and preserves elongated road geometry.

The value of AR >4 as follows the geometric shape of road network. Since road segments are inherently elongated, they exhibit higher aspect ratios, whereas non-road objects such as buildings and noise tend to have compact shapes with lower values of AR. The small holes due to the low spectral variation and fractures in the road network generated by Ostu-based thresholding are filled using morphological operations.

e) Evaluation Metrics: To evaluate the performance of the proposed RNI for road network extraction, the metrics like user's accuracy (UA), producer's accuracy (PA), overall accuracy (OA) and kappa coefficient (KP) are used, which can be calculated as per the following equations.

$$\text{UA} = \frac{TP}{\text{TP+FP}} * 100 \quad (10)$$

$$\text{PA} = \frac{TP}{\text{TP+FN}} * 100 \quad (11)$$

$$\text{OA} = \frac{\text{TP+TN}}{TP+TN+FP+FN} * 100 \quad (12)$$

$$\text{KS} = \frac{P_o - P_e}{1 - P_e} \quad (13)$$

IV. Experimental Results And Discussion

For the development of RNI band selection is a critical task. In this work, spectral analysis is used to identify the bands used for the development of RNI. By selecting specific bands, we can identify the most important ones and minimize the time required for index development. In this work, the NIR and SWIR are used to formulate the RNI. The performance of the proposed method is evaluated on different evaluation metrics, and the Google Earth imagery of the study area is used as reference data for accuracy estimation through in situ observation. The proposed RNI is applied to the TCC Landsat imagery of the study area as shown in Fig. 5 (a) and the initial road extracted by RNI is shown in Fig. 5(b). The initial road network has some false road components eliminated in the post-processing phase using geometric feature analysis and morphological operations, as shown in Fig. 6.

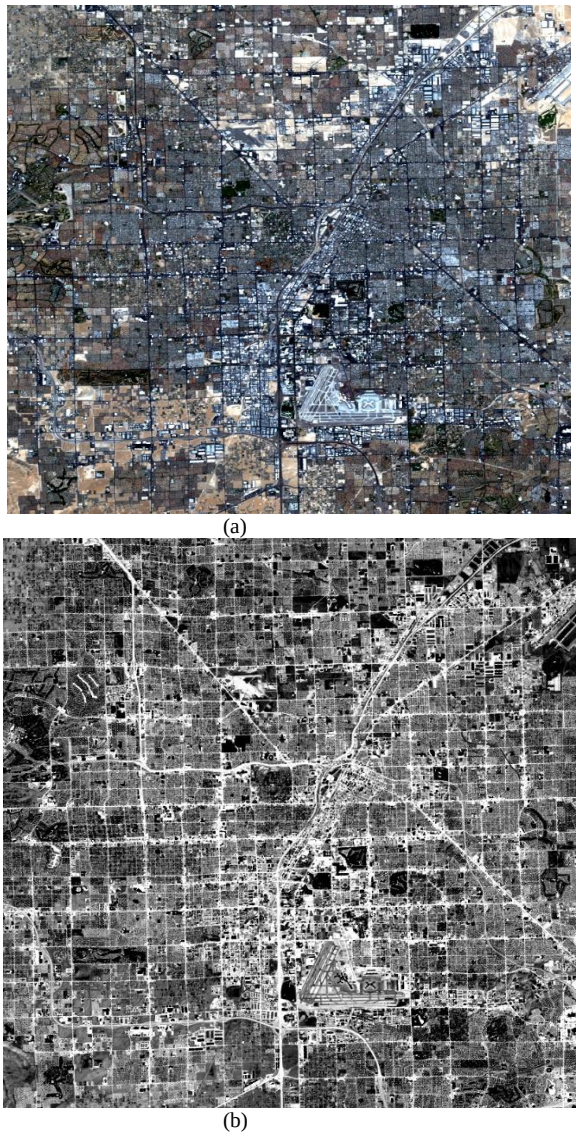

(a)

(b)

Fig. 5. Visualization Road network extracted by RNI (a) TCC Landsat imagery of the study area (b) road network extracted by applying RNI

The final road network obtained by the post-processing step shown in Fig. 6 is complete and accurate, and to assess the performance of the proposed method, different evaluation metrics derived from the confusion matrix, such as UA, PA, OA and KP, are used. For these pixels of each road and non-road classes are selected independently from the training samples to avoid biasness using the stratified random sampling approach across the full study area by matching with the Google Earth imagery of the study area, as shown in Fig. 7, are selected as training and validation samples. The performance of the proposed method on different evaluation metrics is presented in Table II. It has been observed that in the case of the road identification task, the UA is 94.16 % and the PA is 89.15%. Whereas in the case of non-road class, the UA is 89.35% and PA is 94.27%. The OA of the proposed method is 91.67% and in terms of KP parameters which encompasses both UA and PA and denotes the overall performance of the classification as compared to reference data the proposed method has a KP value of 0.8334. The F1-score of 91.64 demonstrated its capability in handling in identifying road pixels in highly complex urban environments.

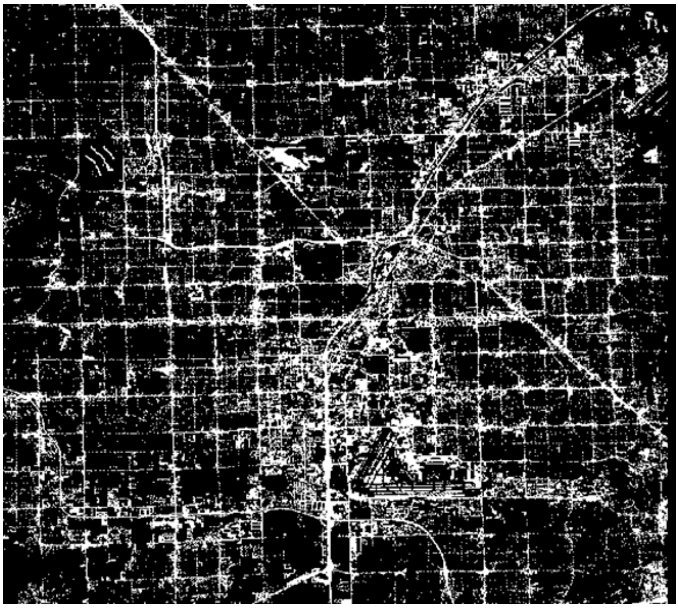

Fig. 6. Road network after eliminating false road components.

TABLE II. ACCURACY ASSESSMENT USING THE CONFUSION MATRIX OF EXTRACTED ROAD NETWORK

Class	***Road***	***Non-Road***	***Total***	***UA***
Road	838	52	890	94.16
Non-Road	102	856	958	89.35
Total	940	908	1848	
PA	89.15	94.27		
OA	91.67			
KS	0.8334			
F1-score	91.64			

Furthermore, the road network extracted by RNI is validated by using Google Earth imagery of the study area, and it has been observed that the road network extracted by RNI is complete, reliable and accurate, as shown in Fig. 7. Although some minor temporal mismatches and geolocation inaccuracies may exist due to differences in sensor geometry and orthorectification processes, these effects are expected to introduce only limited uncertainty in the reported accuracy. The study area has a complex and heterogeneous land cover which makes the road network extraction task more challenging and the presence of various occluding factors and false road components having road-like radiometric properties affects the quality of road extraction. Despite having all the challenges, the road network extracted by the proposed method is acceptable and of high quality. The issue of mixed pixels in the complex urban terrain is handled by emphasizing spectral bands where road materials differ from vegetation and built-up surfaces, allowing partially road-dominated pixels to retain distinguishable index values.

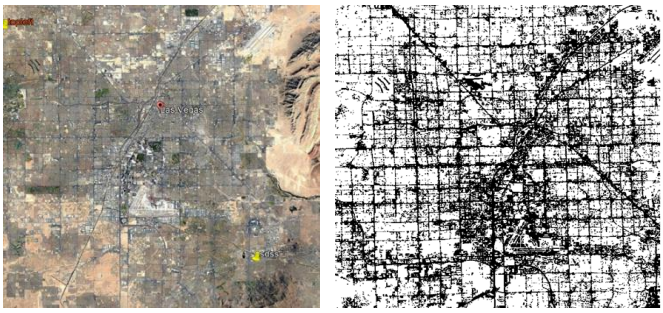

(a) (b)

Fig. 7. Validation of the extracted road network using Google Earth imagery of the study area (a) Google Earth imagery (b) extracted road network.

TABLE III. ACCURACY ASSESSMENT OF EXTRACTED ROAD NETWORK FROM THE IMAGERY OF DIFFERENT TIME PERIOD

Year	***Sensor***	***OA***	***KS***
May, 1990	Landsat-5	78.67	0.7411
May, 2000	Landsat-7	84.14	0.7542
May, 2010	Landsat-7	86.67	0.7516
May 2018	Landsat-8	91.67	0.8334

To assess the robustness and generalization of the proposed method the imagery from different sensors and time periods are used and the extracted road network is shown in Fig. 8 and the performance on different evaluation metric is presented in Table III. On Landsat-5 imagery of the year 1990 an OA of 78.67% and KS of 0.7411 is achieved. While in the year 2000 on Landsat-7 Sensor's imagery the OA increased to 84.14% and KS to 0.7542 and the same growth pattern observed in the imagery of 2010. This increase in road network extraction clearly reflects the urban expansion in the study area which has been continued. These results show that the proposed RNI has performed consistently well across different sensors and time periods which demonstrate the stability and effectiveness of RNI in road network extraction tasks.

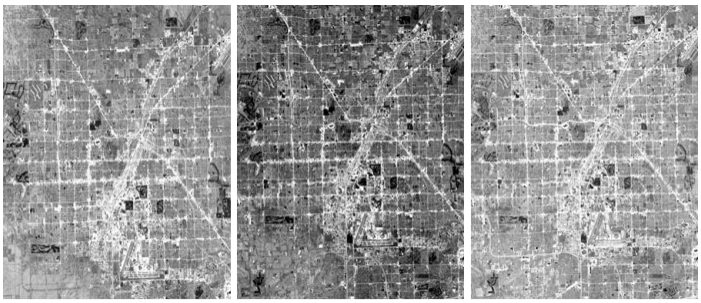

Fig. 8. Visualization of road network extracted by RNI of the study area from images of different years (a) 1990 (b) 2000 (c) 2010.

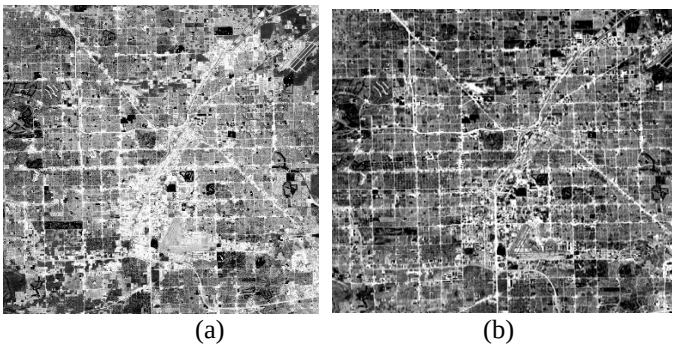

Fig. 9. Road network extracted by the (a) BAI (b) RNI.

V. Comparative Analysis

In this Section the performance of the proposed RNI is matched with existing road network indices (BAI) proposed by Mhangaret al. [31] and the comparative visualization is presented in Fig. 9. Furthermore, the performance of the proposed RNI is not compared with the index REI proposed by Shahi et al.[13] as landsat-8 doesn't have NIR2 band as the author has used world view satellite imagery having different sensors and the index (RI) proposed by RI Reddy et al.[12] is not extracting the heights of the buildings due to complex urban landscape.

The quantitative comparison of the RNI with BAI is presented in Table IV and it has been observed that the proposed that RNI is highly effective in road extraction in the highly populated and structurally complex urban landscape. The RNI has demonstrates consistently superior performance across all evaluation metrics. Specifically, RNI achieves an OA of 91.67%, outperforming BAI by 5.21%, indicating improved pixel-level classification reliability. Furthermore, the KAP of 0.8334 is higher than that of BAI of 0.72, reflecting stronger agreement beyond chance and enhanced accuracy in discriminating road surfaces from spectrally similar urban features. In terms of boundary and shape preservation, RNI attains an F1-score of 91.64 %, significantly exceeding the 84.23% achieved by BAI, highlighting its superior balance between precision and recall. This improvement is particularly critical in densely populated urban areas, where roads are often occluded by buildings, shadows, and heterogeneous materials. The results clearly indicate that RNI is more effective and reliable for extracting continuous and accurate road networks in complex urban environments, making it a suitable choice for large-scale urban road mapping and transportation infrastructure analysis in cities.

TABLE IV. Comparison of RNI with existing road indices

Class	OA	KAP	F1-SCORE
BAI	87.13	0.72	84.23
RNI	91.67	0.8334	91.64

VI. Conclusion

In this work, a novel automated and faster method for generating road maps from multispectral Landsat-8- imagery of densely populated areas using a novel spectral index RNI is presented. For the development of RNI, the significant bands NIR and SWIR are selected using spectral analysis. In spectral analysis, it has been observed that these bands show the highest resemblance to concrete/asphalt material which is primarily used to build roads and other infrastructures. The initial road map generated by RNI has some false roads which are eliminated by geometric feature analysis and morphological operations in the post-processing step. The experimental results reflect that the road network extracted by the proposed method is complete and accurate and in terms of quantitative metrics the method has obtained an accuracy of 91.67%. In the case of the KAP parameter, the proposed method obtained a value of 0.8334. Furthermore, the correctness of the road map identified by the RNI-based method is matched with the Google Earth imagery of the study area. However, the performance of the method deteriorated in cases of low spectral variability and occluded scenes due to shadows of trees and buildings. Despite having these limitations, the proposed RNI-based road network extraction is computationally efficient as it doesn't require large amounts of labelled data for training machine and deep learning models. The main limitation of the RNI is that it will work very well in arid/desert environment not in vegetative areas. This issue can be solved in future works by incorporating other bands in the formation of RNI. In future works the performance of RNI can be tested on other multispectral satellite data or integrating pan-sharpening with the 15 m Panchromatic band of Landsat imagery that could enhance road details

References

[1] J. B. Mena, 'State of the art on automatic road extraction for GIS update: A novel classification', *Pattern Recognit Lett*, vol. 24, no. 16, pp. 3037–3058, 2003, doi: 10.1016/S0167-8655(03)00164-8.

[2] P. P. Singh and R. D. Garg, 'A two-stage framework for road extraction from high-resolution satellite images by using prominent features of impervious surfaces', *Int J Remote Sens*, vol. 35, no. 24, pp. 8074–8107, 2014, doi: 10.1080/01431161.2014.978956.

[3] P. K. Soni, N. Rajpal, and R. Mehta, 'Road Centerline Extraction From VHR Images Using SVM and Multi-Scale Maximum Response Filter', *Journal of the Indian Society of Remote Sensing*, vol. 49, no. 7, pp. 1519–1532, 2021, doi: 10.1007/s12524-021-01329-2.

[4] C. Robinson *et al*., 'Large scale high-resolution land cover mapping with multi-resolution data', in *Proceedings of the IEEE/CVF Conference on Computer Vision and Pattern Recognition*, 2019, pp. 12726–12735.

[5] M. J. Khan and P. P. Singh, 'Advanced road extraction using CNN-based U-Net model and satellite imagery', *e-Prime - Advances in Electrical Engineering, Electronics and Energy*, vol. 5, p. 100244, 2023, doi: https://doi.org/10.1016/j.prime.2023.100244.

[6] A. Abdollahi, B. Pradhan, and N. Shukla, 'Road Extraction from High-Resolution Orthophoto Images Using Convolutional Neural Network', *Journal of the Indian Society of Remote Sensing*, vol. 49, no. 3, pp. 569–583, 2021, doi: 10.1007/s12524-020-01228-y.

[7] M. Drusch *et al.*, 'Sentinel-2: ESA's Optical High-Resolution Mission for GMES Operational Services', *Remote Sens Environ*, vol. 120, pp. 25–36, 2012, doi: https://doi.org/10.1016/j.rse.2011.11.026.

[8] S. L. K. Reddy, C. V. Rao, P. Rajesh Kumar, R. V. G. Anjaneyulu, and B. Gopala Krishna, 'An index based road feature extraction from LANDSAT-8 OLI images', *International Journal of Electrical and Computer Engineering*, vol. 11, no. 2, pp. 1319–1336, Apr. 2021, doi: 10.11591/ijece.v11i2.pp1319-1336.

[9] Y. Jia, X. Zhang, R. Xiang, and Y. Ge, 'Super-Resolution Rural Road Extraction from Sentinel-2 Imagery Using a Spatial Relationship-Informed Network', *Remote Sens (Basel)*, vol. 15, no. 17, 2023, doi: 10.3390/rs15174193.

[10] Y. Khurana, P. K. Soni, and D. P. Bhatt, 'SVM-based classification of multi-temporal Sentinel-2 imagery of dense urban land cover of Delhi-NCR region', *Earth Sci Inform*, vol. 16, no. 2, pp. 1765–1777, 2023, doi: 10.1007/s12145-023-01008-5.

[11] Y. Hu and K. J. Zu, 'Road extraction from remote sensing imagery based on road tracking and ribbon snake', in *KESE 2009 - 2009 Pacific-Asia Conference on Knowledge Engineering and Software Engineering*, 2009, pp. 201–204. doi: 10.1109/KESE.2009.60.

[12] S. L. K. Reddy, C. V Rao, P. R. Kumar, R. V. G. Anjaneyulu, and B. G. Krishna, 'An index based road feature extraction from LANDSAT-8 OLI images', *International Journal of Electrical and Computer Engineering*, vol. 11, no. 2, p. 1319, 2021.

[13] K. Shahi, H. Z. M. Shafri, E. Taherzadeh, S. Mansor, and R. Muniandy, 'A novel spectral index to automatically extract road networks from WorldView-2 satellite imagery', *The Egyptian Journal of Remote Sensing and Space Science*, vol. 18, no. 1, pp. 27–33, 2015, doi: https://doi.org/10.1016/j.ejrs.2014.12.003.

[14] X. G. Y. Y. X. X. Kun Jia Xiangqin Wei and B. Li, 'Land cover classification using Landsat 8 Operational Land Imager data in Beijing, China', *Geocarto Int*, vol. 29, no. 8, pp. 941–951, 2014, doi: 10.1080/10106049.2014.894586.

[15] P. K. Soni, N. Rajpal, R. Mehta, and V. K. Mishra, 'Urban land cover and land use classification using multispectral sentinal-2 imagery', *Multimed Tools Appl*, 2021, doi: 10.1007/s11042-021-10991-0.

[16] V. F. Rodriguez-Galiano, M. Chica-Olmo, F. Abarca-Hernandez, P. M. Atkinson, and C. Jeganathan, 'Random Forest classification of Mediterranean land cover using multi-seasonal imagery and multi-seasonal texture', *Remote Sens Environ*, vol. 121, pp. 93–107, 2012, doi: https://doi.org/10.1016/j.rse.2011.12.003.

[17] M. Singh and K. D. Tyagi, 'Pixel based classification for Landsat 8 OLI multispectral satellite images using deep learning neural network', *Remote Sens Appl*, vol. 24, p. 100645, 2021, doi: https://doi.org/10.1016/j.rsase.2021.100645.

[18] B. Slagter *et al.*, 'Monitoring road development in Congo Basin forests with multi-sensor satellite imagery and deep learning', *Remote Sens Environ*, p. 114380, 2024, doi: https://doi.org/10.1016/j.rse.2024.114380.

[19] Z. Xu, K. Guan, N. Casler, B. Peng, and S. Wang, 'A 3D convolutional neural network method for land cover classification using LiDAR and multi-temporal Landsat imagery', *ISPRS Journal of Photogrammetry and Remote Sensing*, vol. 144, pp. 423–434, 2018, doi: https://doi.org/10.1016/j.isprsjprs.2018.08.005.

[20] R. Lian, W. Wang, N. Mustafa, and L. Huang, 'Road extraction methods in high-resolution remote sensing images: A comprehensive review', *IEEE J Sel Top Appl Earth Obs Remote Sens*, vol. 13, pp. 5489–5507, 2020, doi: 10.1109/JSTARS.2020.3023549.

[21] A. Gruen and H. Li, 'Semi-automatic linear feature extraction by dynamic programming and LSB-snakes', *Photogramm Eng Remote Sensing*, vol. 63, no. 8, pp. 985–994, 1997.

[22] A. P. Dal Poz, R. B. Zanin, and G. M. do Vale, 'Automated extraction of road network from medium-and high-resolution images', *Pattern Recognition and Image Analysis*, vol. 16, no. 2, pp. 239–248, 2006, doi: 10.1134/S1054661806020118.

[23] D. Herumurti, K. Uchimura, G. Koutaki, and T. Uemura, 'Urban road extraction based on hough transform and region growing', in *Frontiers of Computer Vision,(FCV), 2013 19th Korea-Japan Joint Workshop on*, 2013, pp. 220–224.

[24] H. R. R. Bakhtiari, A. Abdollahi, and H. Rezaeian, 'Semi automatic road extraction from digital images', *Egyptian Journal of Remote Sensing and Space Science*, vol. 20, no. 1, pp. 117–123, 2017, doi: 10.1016/j.ejrs.2017.03.001.

[25] L. Risser, F. Plouraboue, and X. Descombes, 'Gap Filling of 3-D Microvascular Networks by Tensor Voting', *IEEE Trans Med Imaging*, vol. 27, no. 5, pp. 674–687, 2008, doi: 10.1109/TMI.2007.913248.

[26] P. N. Anil and S. Natarajan, 'Road Extraction Using Topological Derivative and Mathematical Morphology', *Journal of the Indian Society of Remote Sensing*, vol. 41, no. 3, pp. 719–724, 2013, doi: 10.1007/s12524-012-0231-6.

[27] R. Liu, J. Song, Q. Miao, P. Xu, and Q. Xue, 'Road centerlines extraction from high resolution images based on an improved directional segmentation and road probability', *Neurocomputing*, vol. 212, pp. 88–95, 2016, doi: 10.1016/j.neucom.2016.03.095.

[28] W. Shi, Z. Miao, and J. Debayle, 'An integrated method for urban main-road centerline extraction from optical remotely sensed imagery', *IEEE Transactions on Geoscience and Remote Sensing*, vol. 52, no. 6, pp. 3359–3372, 2014, doi: 10.1109/TGRS.2013.2272593.

[29] F. E. L. J. G. Masek and S. N. Goward, 'Dynamics of urban growth in the Washington DC metropolitan area, 1973-1996, from Landsat observations', *Int J Remote Sens*, vol. 21, no. 18, pp. 3473–3486, 2000, doi: 10.1080/014311600750037507.

[30] J. G. Y. Zha and S. Ni, 'Use of normalized difference built-up index in automatically mapping urban areas from TM imagery', *Int J Remote Sens*, vol. 24, no. 3, pp. 583–594, 2003, doi: 10.1080/01431160304987.

[31] P. Mhangara, J. Odindi, L. Kleyn, and H. Remas, 'Road extraction using object oriented classification', *Visualisation technical*, pp. 45–50, 2011.

[32] M. W. Ahmed, S. Saadi, and M. Ahmed, 'Automated road extraction using reinforced road indices for Sentinel-2 data', *Array*, vol. 16, p. 100257, 2022, doi: https://doi.org/10.1016/j.array.2022.100257.

[33] N. Otsu, 'A threshold selection method from gray-level histograms', *IEEE Trans Syst Man Cybern*, vol. 9, no. 1, pp. 62–66, 1979.

[34] P. K. Soni, N. Rajpal, and R. Mehta, 'Semiautomatic Road Extraction Framework Based on Shape Features and LS-SVM from High-Resolution Images', *Journal of the Indian Society of Remote Sensing*, vol. 48, no. 3, pp. 513–524, 2020, doi: 10.1007/s12524-019-01077-4.